Wideband OFDM System for Radar and Communications

Dmitriy Garmatyuk
Department of ECE
Miami University
Oxford, OH USA
garmatd@muohio.edu

Kyle Kauffman
Department of Computer Science/Department of ECE
Miami University
Oxford, OH USA
kauffmkj@muohio.edu

Jonathan Schuerger
Department of Physics/Department of ECE
Miami University
Oxford, OH USA
schuerjp@muohio.edu

Scott Spalding
Department of ECE
Miami University
Oxford, OH USA
spaldisa@muohio.edu

***Abstract*— This paper describes the design and architectural composition of a radar system built on OFDM platform. The radar signal is generated digitally by forming an arbitrary-length vector of OFDM sub-carrier amplitudes and translating it in analog format via 1000 Ms/s D/A conversion. The resultant baseband signal has a bandwidth of 500 MHz, and variable number and composition of sub-carriers, which may be changed on a pulse-to-pulse basis. The signal is upconverted to 7.5 GHz carrier frequency and emitted via small-form horn antenna. The receiver includes 1 Gs/s A/D converter and processing is performed in frequency domain. The system is currently configured for short-range applications (3-5 m) and can be used as radar or communication unit without any changes to hardware and with very minimal changes to software. Experimental results from high-resolution range profile imaging and broadband data communications are presented and discussed.**

I. INTRODUCTION

The concept of miniaturized, potentially dual-use (radar/communication), high-resolution all-weather imaging sensor can be addressed from several different perspectives [1, 2]; the purpose of this paper is to suggest the solution via utilizing UWB orthogonal frequency division multiplexing (OFDM) system architecture and wave-forming method. OFDM as a method of digital modulation is not a new technique – its concept was explored in 1960's by several researchers, e.g. [3]. However, it was not until the beginning of the 2000's that this technique and corresponding system architecture started being considered for wideband applications. There were two major reasons precluding UWB implementation of OFDM: Federal Communications Commission's (FCC) ban on commercial use of wide swaths of spectrum, which was lifted for extremely low-power signals in 2002; and unavailability of fast, inexpensive analog-to-digital (A/D) and digital-to-analog (D/A) converters [4], as they are significant components of an OFDM system determining its bandwidth. As soon as these two hurdles were overcome, UWB OFDM became a focus of R&D efforts in the industry and academia with an emphasis on commercial broadband communications [5, 6].

Implementation of OFDM signals and system architecture in radar, on the other hand, has not been as widely explored as in communications. Most notable research work concerning OFDM-coded radar signals is by Dr. Nadav Levanon, whose analyses of multicarrier phase coded (MCPC) radar signal performance were based on OFDM signal construction [7, 8]. Another study of OFDM-coded radar signals, published in [9], pointed out that these signals compare favorably to same-bandwidth LFM waveforms since range-Doppler coupling/ambiguity is much less pronounced in case of using OFDM signals.

Despite fairly significant advantages – such as pulse diversity potential and dual-use system design – OFDM, and, in particular, UWB OFDM signal construction and system architecture were not previously considered for applications in imaging radar. This paper is intended as initial analysis of such an application, examined from experimental perspective.

This work is supported by the U.S. Air Force Office of Scientific Research under Grant FA9550-07-1-0297.

978-1-4244-2871-7/09/$25.00 ©2009 IEEE

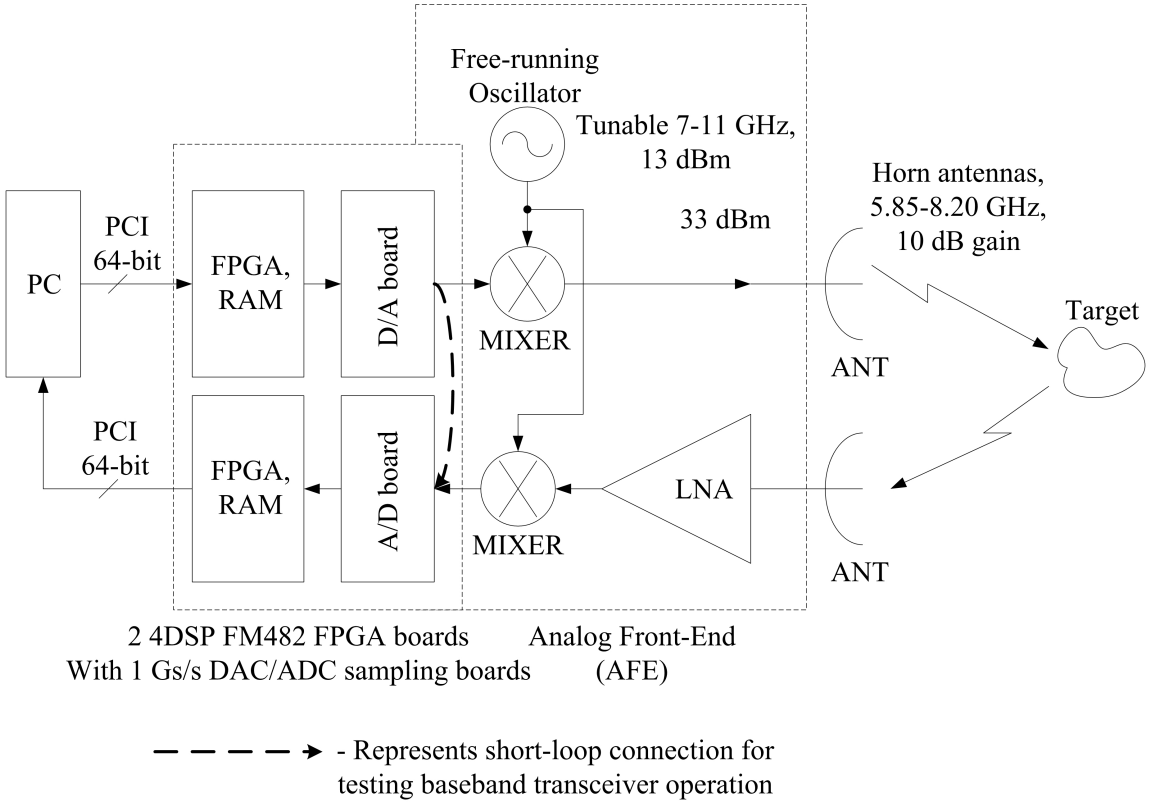

Figure 1. Block diagram of the designed OFDM system.

II. System Description

The system is built as a short-range, high-resolution radar and communication unit for possible implementation in airborne sensor networks. OFDM signal construction is performed in the digital block and the subsequent upconversion and amplification is performed in the analog front-end (AFE) portion, as shown in Fig. 1.

OFDM signal is comprised of the N sub-carriers (sub-bands), which are represented as a vector of frequency-domain components, populated by the desired code pattern.

If we select a ternary alphabet $\{0, \pm 1\}$ for populating these components, the signal in sample domain can then be represented as –

$$x(n) = \frac{1}{2N+1} \sum_{k=1}^{2N+1} X(k) \cdot \cos\left(2\pi \frac{(k-1)(n-1)}{2N+1}\right), \quad \text{for } n \in [1,\ 2N+1] \tag{1}$$

where n is the index of a time-domain sample and $X(k)$ are values of a frequency-domain vector selected from a ternary alphabet either randomly, or according to a desired code combination.

The translation of sample-value signal vector $\boldsymbol{s}$ from sample domain to an electrical signal is performed using D/A converter, which is a crucial component of OFDM architecture. Assuming a certain conversion speed L samples per second we can deduce time and frequency characteristics of the output signal. From (1) it is evident that the wave is a sum of cosine RF pulses, each of duration 2N/L seconds, which is the duration of entire OFDM pulse, too. Further examining (1) we can see that the nth cosine pulse, if plotted for all k's from 1 to 2N+1, has exactly n periods within the time duration of OFDM pulse. This allows us to calculate each individual pulse's physical frequency and, thus, determine its spectrum's location on the frequency axis. We then observe that the described method, indeed, produced a signal with multiple sub-bands which are orthogonal to each other in that the peak of any sub-band's sinc-function spectrum coincides with zeros of all other sub-band spectra, as shown in Figure 2. If sampling frequency of D/A converter is $F_s = 1/T$ we can write the baseband transmit signal as (2).

It is also possible to infer that the overall useful bandwidth of baseband OFDM signal is equal to half the sampling rate of D/A converter and is not dependent on any other factors (such as number of sub-bands). This observation also explains why UWB OFDM systems were not implemented earlier, as stated

in the Introduction. It also adds to the list of UWB OFDM benefits the advantage of scalability, as implementing a faster D/A and A/D converters would allow to instantly upgrade the resolution of such a radar system. Thus, simplest UWB OFDM wave-shaping system can consist of only two major blocks – IFFT digital module and D/A converter.

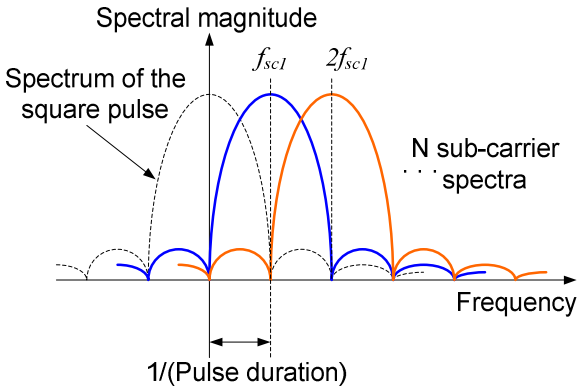

Figure 2. OFDM signal spectrum illustration.

$$x(t)=\frac{1}{2N+1}\sum_{n=1}^{2N+1}\sum_{k=1}^{2N+1}X(k)\cdot\left(\cos\left(2\pi\frac{(k-1)(n-1)}{2N+1}\right)\cdot\delta(t-nT)\right), \quad (2)$$

where $\delta(t)$ is Dirac delta function.

Table I below details the parameters of the current system and lists performance characteristics.

TABLE I. OFDM SYSTEM PARAMETERS

Parameter	Value	Units
Baseband signal bandwidth	500	MHz
Transmitted signal bandwidth	7.0…8.0	GHz
Standard pulse width	513	ns
Transmit power, approximately	25	mW
Experimental radar range, as tested	1.5…5	meters
Number of bits in commun. configuration	19	Per pulse
Experimental range resolution	0.30	meter

III. EXPERIMENTAL DATA

The digital portion of the system was tested first to ensure random OFDM radar waveforms can be correctly generated. The signal data (i.e. time domain samples) are generated in MATLAB and sent directly to a transmitter board via a PCI bus. The data are converted into analog format at 1 Gs/s speed. All signals are scaled to remain within the amplitude limits of the D/A converter. The waveform is sent directly to the receiver board and/or AFE using mini-SMA connectors, thus enabling easy interface to subsequent radar AFE components. The SMA cable connection between the transmitter and receiver is approximately 1 meter. All SMA connections are such that the output waveform can be sent directly to the receiver, through the radar, or both simultaneously. Each element (i.e. sub-band) in the vector is a normally distributed random variable with zero mean and variance of one – which still conforms to the general format of the signal in (2), only with non-integer, real-valued coefficients *X(k)*. The bandwidth of an OFDM waveform is limited only by the D/A converter, therefore, the Nyquist-rate sampling at 1 Gs/s allows for a usable signal bandwidth of 500 MHz. The bandwidth of the signal will remain the same for any number of sub-bands used when generating the waveform.

A. Direct Transmitter-Receiver Loop

To estimate the goodness of the D/A and A/D conversion, the received sampled OFDM signal was cross-correlated with the MATLAB simulated transmit signal. Fig. 3(a) and (b) show the MATLAB randomly generated OFDM waveform with 256 sub-bands and the received waveform respectively. Fig. 3(c) shows the cross-correlation of those two signals. As can be seen in it the difference in the peak and highest sidelobe is approximately 15 dB, which is deemed satisfactory for system prototype implementation. The result can be improved by conditioning the OFDM waveform in the AFE and/or by reducing the peak-to-average power ration (PAPR) through control of sub-band distribution during signal generation.

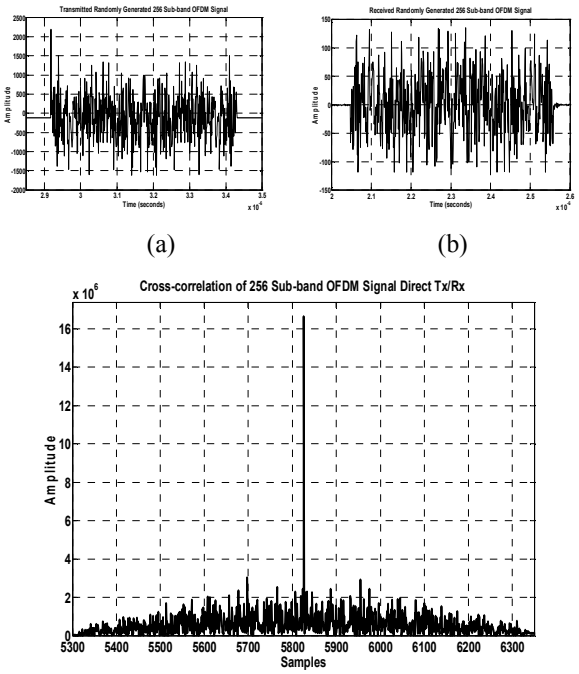

Figure 3. Direct-loop experiment results: (a) Original OFDM pulse generated in MATLAB; (b) Received signal recorded from the A/D converter; (c) Cross-correlation between the original and received signals.

B. Range Profile Experiment

The test objectives are to construct a range profile for a multiple number of targets and determine the resolution of the current system. The targets used in experimentation were trihedral corner reflectors with 1-foot square sides, resulting in an RCS of approximately 2 m^2. Estimated signal power at the target is about −30 dBm, which is compliant with the FCC spectral mask for UWB-OFDM transmissions. Indoor short-range experiments were conducted and it was determined that a target placement of above approximately 1.1 meters from the antennas would allow for far field testing. Range profiles were obtained via matched filtering of original simulated signals and received sampled signals. Four separate tests were conducted:

- Transmission and reception of OFDM waveforms with no targets present. Check cross-correlation to ensure only noise was received.
- Transmission and reception of OFDM waveforms with only one target present. Check matched filtered response to ensure target detection and generate target range profile.
- Transmission and reception of OFDM waveforms with two targets present. Obtain range profiles for varying target distances and ensure that the actual target separation matches the distance in the range profile. Determine system resolution.
- Transmission and reception of OFDM waveforms with three targets present. Obtain range profiles for varying target distances and ensure that the actual target separation matches the distance in the range profile.

For the first test the target resided 1.57 meters from the radar antennas. Fig. 4 shows the obtained range profile for this scenario. The difference from peak to the highest sidelobe is approximately 17 dB which is 2dB better than direct transmission to the receiver. This improvement may seem surprising; however, the random nature of the signal will cause the difference to vary for every transmission. Again, this can be controlled through sub-band manipulation.

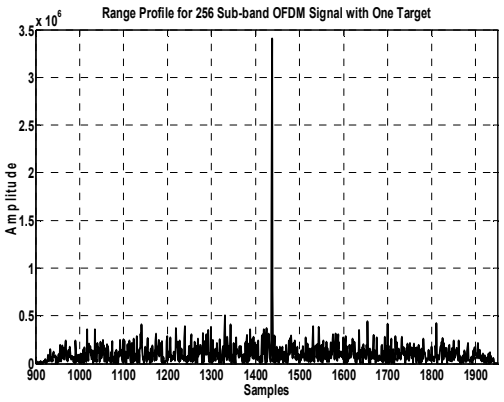

Figure 4. Single target test result for a 256-sub-band OFDM signal with randomly distributed sub-band coefficients and the target located 1.57 meters from the transmit/receive antennas.

In the third scenario we introduced a second target to the target area. Both targets were identical corner reflectors with the same 2 m^2 RCS each. The first target was, again, located 1.57 meters from the radar antennas. The distance of the second target was varied with respect to the first target and several range profiles were obtained. The receiver A/D converter records one sample every sample period Δt which, in our case, is 1 nanosecond. Therefore, we calculate the theoretical range bin resolution as

$$\Delta x = \frac{c \cdot \Delta t}{2} = 0.15\ m \tag{3}$$

This states that two targets must be a minimum of $2\Delta x$ = .30 meters apart to be successfully discerned. Table II shows the experimental parameters for several different locations of the second target. It is seen that the error in determining distance between the two targets does not exceed 2 cm and the error in determining the range to the nearest target does not exceed 10 cm.

TABLE II. TWO-TARGET RANGE PROFILE DATA

Fig. 5 graph	**Actual distance, m (From antennas/From 1st target)**	**Recovered distance, m (From antennas/From 1st target)**
(a)	1.85/0.28	1.95/0.30
(b)	2.00/0.43	2.10/0.45
(c)	2.16/0.59	2.25/0.60
(d)	2.61/1.04	2.70/1.05

Fig. 5(a)-(d) show the range profiles for the two target scenario corresponding to Table II. All of the range profiles are magnified at the peaks so the number of samples between peaks can be seen more clearly. To determine the actual target range we sent the transmit signal directly to the receiver using short-loop path, while simultaneously sending it through the radar AFE to the antennas. We then performed matched filtering of the transmitted and received signals using the first peak as the reference point, measuring the number of samples between the reference peak and the target peak. Using the expected number of time samples for the signal traveling from the antenna to the target we can determine the signal travel time through the radar AFE and cables by subtraction of the samples. Adopting this technique, we have determined that the front end delay is 26 samples or 26 nanoseconds. Notice in Fig. 5(a) that the two peaks are distinguishable and the number of samples between peaks is two, which matches the expected resolution limit of 0.30 meters.

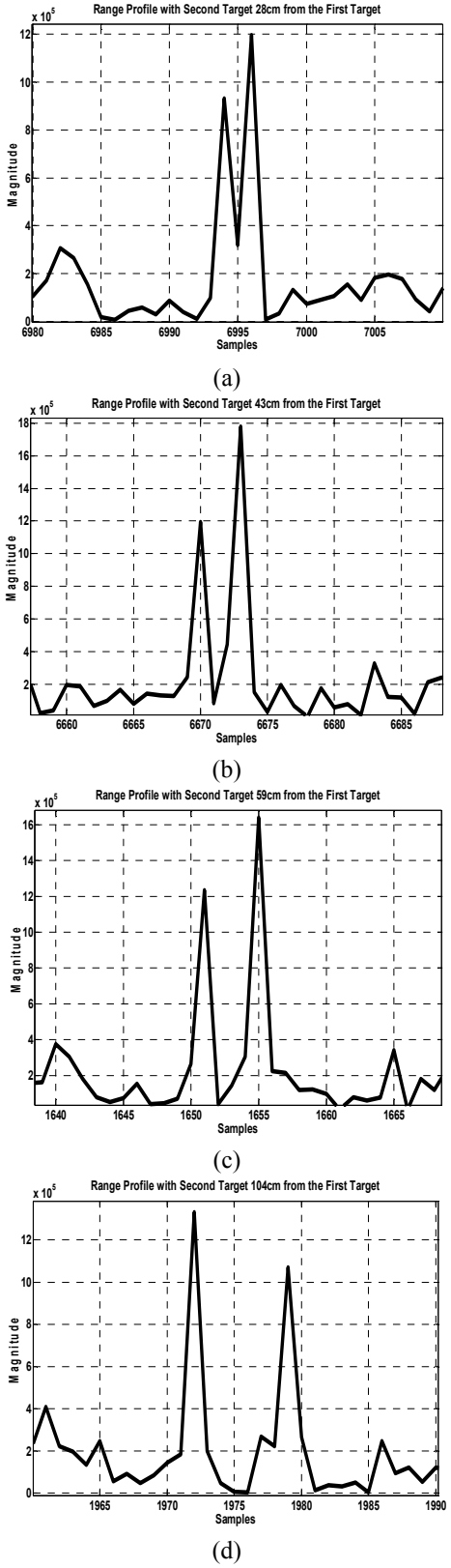

Figure 5. Two-target test result for a 256-sub-band OFDM signal with randomly distributed sub-band coefficients, with two targets being apart by: (a) 0.28 m; (b) 0.43 m; (c) 0.59 m; (d) 1.04 m.

C. Data Communication Experiment

The goal of this experiment is to show that the designed system can be used as a broadband data communication device with no hardware adjustments. Communications using the radar requires the identification of which sub-bands are enabled upon receipt of the OFDM symbol. The transmission speed depends on the number of sub-bands (sub-channels) that can be simultaneously enabled. The B = 500 MHz bandwidth of the baseband signal is sub-divided into C sub-channels. The OFDM symbol is formed by taking the IFFT of the data vector encoded in frequency domain, forming a set of $2C$ samples. Since the symbol generation is software defined, the number of sub-channels may be dynamically set in real time to account for varying channel considerations. For the experiments in this section, the number of sub-channels was chosen to be 64. Thus, each OFDM symbol has length

$$L_{sym} = \frac{2 \cdot C}{2 \cdot B} = 128\,ns \tag{4}$$

The binary serial input data is divided into blocks of length C. Each block is encoded by mapping the block's bits onto the sub-channels of the OFDM symbol. The sub-channels were modulated using on-off keying (OOK) to facilitate easier data recovery. OOK encodes one bit per channel, so each input data block maps directly to one OFDM symbol. With all of the 64 sub-carriers enabled a maximum bit/symbol rate of 64 could be achieved. Experimentally it was found that many of the physical channels were susceptible to systemic in-band noise generated by the AFE, and thus a subset of size $C_{enabled}$ of the physical channels C was chosen to carry data during our tests. PAPR issues were mitigated by standard clipping techniques [10].

The guard interval between successive OFDM symbols was chosen to be 4 times the length of the typical delay spread of UWB signals in our environment [11], resulting in a guard interval length of L_{guard} = 200 ns.

The low $\frac{L_{sym}}{L_{guard}}$ ratio infers an efficiency loss in data rate; however, the small L_{sym} was chosen to decrease the PRI for increased jamming resistance of system operation. The data rate of our system is then

$$R = \frac{C_{enabled}}{L_{guard} + L_{sym}} \tag{5}$$

Initial tests found that the A/D converter in the receiver block injected high frequency/magnitude noise into the received time-domain sample data set, as shown in Fig. 6(a). This noise is only injected at time samples where a high-amplitude signal is not present, and thus is prone to time-domain filtering. The filtering process used heuristics to

identify high frequency oscillatory behavior and zeroed out affected samples, leaving the OFDM signal unmodified, as shown in Fig. 6(b).

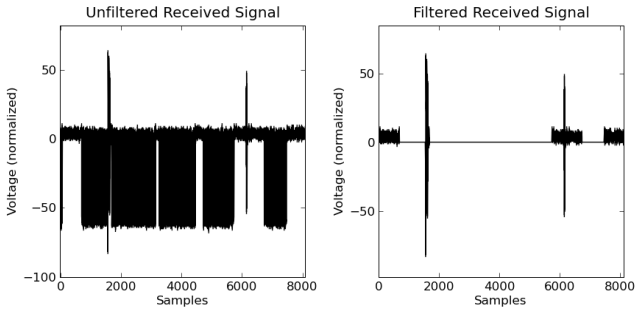

Figure 6. Raw and filtered received OFDM signal data: (a) Unfiltered; (b) Filtered using high-frequency harmonic noise rejection.

Experimentally it was found that sub-channels in the 0-100 MHz range, as well as those near the sampling rate in 470-500 MHz range, interfered heavily with the operation of nearby sub-channels. This effect is due to signal distortion by the D/A and A/D conversions, and it is not an effect of the transmission channel. To reduce this ICI, guard bands equal to the width of a single channel were introduced to reduce the effect of energy spreading on adjacent bands. In addition, sub-carriers that were prone to ICI were not used for data transmission and were also treated as guard bands. This approach is found to be reasonably resilient to adjacent band ICI. Three configurations of enabled sub-channels were tested, as shown in Table III.

TABLE III. SUB-CHANNEL CONFIGURATIONS

Config.	**Enabled sub-channels**	**Total number of sub-channels**	**Resultant data rate, Mb/s**
C1	16-60, even only	19	57
C2	10-60, even only	26	79
C3	0-64, even only	32	97

The system was characterized in all three configurations by transmission and recovery of a 16x16 monochrome printer icon to visualize actual data transfer. The distance between transmit and receive antennas was approximately 4.5 meters. The received images in each of C1-C3 configurations are shown in Fig. 7. It is seen that the system's current data rate limit is between 79 and 97 Mb/s.

IV. CONCLUSION

An experimental system based on OFDM architecture has been designed and built at Miami University. The system's useful bandwidth is 500 MHz, which allows it to perform as high-resolution radar with range resolution approximately 0.30 meter. The system can also be used as a communication unit with experimental data rate of 57 Mb/s enabling image communications. There are no required hardware alterations to make the system switch from radar to communications functionality and only minor software adjustments are necessary. The system is also expected to possess good anti-jamming capabilities by employing pulse diversity due to the ability to change the number and composition of sub-carriers, as well as pulse width on a pulse-to-pulse basis. Implementation of such a system is targeted at low cost/weight airborne platforms in radar sensor network environments.

(a) (b) (c)

Figure 7. 16x16 monochrome image transmission at 4.5 meter distance results: (a) At 57 Mb/s (ideal image); (b) At 79 Mb/s; (c) At 97 Mb/s.

REFERENCES

[1] *Sandia MiniSAR – Miniaturized Synthetic Aperture Radar*, Sandia National Laboratories, Albuquerque, NM. Available: http://www.sandia.gov/RADAR/minisar.html

[2] M. Edrich, "Ultra-lightweight synthetic aperture radar based on a 35 GHz FMCW sensor concept and online raw data transmission," in *IEE Proc. Radar, Sonar Navig.*, vol. 153, pp. 129–134, Apr. 2006.

[3] R. Chang and R. Gibby, "A theoretical study of performance of an orthogonal multiplexing data transmission scheme," *IEEE Trans. Communications,* vol. 16, no. 4, pp. 529–540, Aug. 1968.

[4] Bin Le, T. W. Rondeau, J. H. Reed, and C. W. Bostian, "Analog-to-digital converters," *IEEE Signal Processing Mag.*, vol. 22, no. 6, pp. 69–77, Nov. 2005.

[5] A. Batra, J. Balakrishnan, G. R. Aiello, J. R. Foerster, and A. Dabak, "Design of a multiband OFDM system for realistic UWB channel environments," *IEEE Trans. Microwave Theory and Tech.*, vol. 52, no. 9, Part 1, pp. 2123–2138, Sep. 2004.

[6] C. Snow, L. Lampe, and R. Schober, "Performance analysis of multiband OFDM for UWB communication," in *Proc. 2005 IEEE Int. Conf. Communications*, Seoul, Korea, 2005, vol. 4, pp. 2573–2578.

[7] N. Levanon, "Multifrequency complementary phase-coded radar signal," in *IEE Proc. Radar, Sonar Navig.*, vol. 147, no. 6, pp. 276–284, Dec. 2000.

[8] N. Levanon and E. Mozeson, *Radar Signals.* Hoboken, NJ: Wiley-Interscience, 2004, ch. 11.

[9] G. E. A. Franken, H. Nikookar, and P. van Genderen, "Doppler tolerance of OFDM-coded radar signals," in *Proc. 2006 European Radar Conf.*, Manchester, UK, 2005, pp. 108–111.

[10] Xiaodong Li, L.J. Cimini, Jr., "Effects of clipping and filtering on the performance of OFDM," in Proc. *1997 IEEE 47th Vehicular Technology Conf.*, Phoenix, AZ, 1997, vol.3, pp.1634–1638.

[11] T.Jamsa, V.Hovinen, A.Karjalainen, J. Iinatti, "Frequency dependency of delay spread and path loss in indoor ultra-wideband channels," in Proc. *2006 Institution of Engineering and Technology Seminar on Ultra Wideband Syst., Tech. and App.*, London, UK, 2006, pp.254–258.